Dual-band OOFDM system based on tandem single-sideband modulation transmitter

Zhenbo Xu, [1] Rongqing Hui[1*], and Maurice O'Sullivan[2]

[1] *Information & Telecommunication Technology Center, the University of Kansas, Lawrence, KS 66045, USA*
[2] *Nortel, Ottawa Carling Campus, 3500 Carling Ave., Nepean, ON, K2H 8E9, Canada*
rhui@ku.edu

Abstract: We demonstrate an optical orthogonal frequency division multiplex (OOFDM) transmitter using a simple dual-electrode Mach-Zehnder modulator (MZM) to perform tandem single-sideband optical modulation. This allows a doubling of transmission capacity. A commercial optical transmitter card, equipped with an on-board arbitrary waveform generator, is used for the system test. A proof-of-concept transmission experiment is conducted using a fiber-optic re-circulating loop.

OCIS codes: (060.4080) Modulation; (060.0060) Fiber optics and optical communications; (060 2360) Fiber optics link and subsystems; (060 2630) Frequency modulation

---

References and links

1. R. V. Nee, and R. Prasad, *OFDM for Wireless Multimedia Communications* (Artech House Publishers 2000).
2. L. Hanzo, and T. Keller, *OFDM and MC-CDMA A Primer (*John Wiley 2006).
3. T. D. Chiueh, and P. Y. Tsai, *OFDM Baseband Receiver Design of Wireless Communications* (Wiley Press 2007).
4. J. Armstrong, "OFDM for Optical Communications," J. Lightwave Technol. **27** 189-204 (2009).
5. I. B. Djordjevic, and B. Vasic, "Orthogonal Frequency Division Multiplexing for High-speed Optical Transmission," Opt. Express **14**, 3767-3775 (2006).
6. W. Shieh, H. Bao, and Y. Tang, "Coherent Optical OFDM: theory and design," Opt. Express **16**, 841-859 (2008).
7. W. Shieh, X. Yi, Y. Ma, and Q. Yang, "Coherent optical OFDM: has its time come?" Opt. Express **7**, 234-255 (2008).
8. A. J. Lowery, and J. Armstrong, "Orthogonal-frequency-division multiplexing for dispersion compensation of long-haul optical systems," Opt. Express **14,** 2079-2084 (2006).
9. A. J. Lowery, L. B. Du, and J. Armstrong, "Performance of Optical OFDM Ultralong-Haul WDM Lightwave Systems," J. Lightwave Technol. **25**, 131-138 (2007). in
10. Brendon J.C. Schmidt, A. Lowery, and J. Armstrong, "Experimental Demonstration of Electronic Dispersion Compensation for Long-Haul Transmission Using Direct-Detection Optical OFDM," J. Lightwave Technol. **26**, 196-203 (2008).
11. S. C. Lee, F. Breyer, S. Randel, etc, "24Gb/s transmission over 730m of Multimode Fiber by Direct Modulation of an 850nm VCSEL using discrete Mult-tone Modulation," in Proc OFC, paper PDP6 (2007).
12. S. Jansen, I. Morita, N. Takeda, and H. Tanaka, "20Gb/s OFDM Transmission over 4160km SSMF Enabled by FR-Pilot Phase Noise Compensation," in Proc OFC*,* Paper PDP15 (2007).
13. Y. Benlanchtar. G. Gavioli, V. Mikhailov, and R. Killy, "Experimental investigation of SPM in long- haul direct-detection OFDM systems," Opt. Express **16**, 15477-15482 (2008).
14. S. Jansen, I. Morita, T. W. Schenk, N. Takeda, and H. Tanaka, "Coherent Optical 25.8Gb/s OFDM Transmission Over 4160km SSMF," J. Lightwave Technol. **26**, 6-15 (2008).
15. Y. Ma, Q. Yang, Y. Tang, S. Chen, and W. Shieh, "1-Tb/s per Channel Coherent Optical OFDM Transmission with Subwavelength Bandwidth Access," in Proc OFC, paper PDPC1 (2009).
16. S. Jansen, I. Morita, T. Schenk, and H. Tanaka, "121.9 Gb/s PDM-OFDM transmission with 2b/s/Hz Spectral Efficiency over 1000km of SSMF," J. Lightwave Technol. **27**, 177-188 (2009).
17. B. J. C. Schmidt, A. J. Lowery, and J. Armstrong, "Experimental Demonstration of 20Gb/s Direct-Detection Optical OFDM and 12Gb.s with a colorless transmitter," in Proc OFC, PDP 18 (2007).
18. G. H. Smith, D. Novak, and Z. Ahmed, **"**Technique for optical SSB generation to overcome dispersionpenalties in fibre-radio systems**,"** IEE Electron. Lett. **33,** 74-75 (1997)
19. R. Hui, "Multi-tributary OFDM Optical Transmitter Using Carrier-Suppressed Optical Single-Sideband Modulation," in Proc OFC, paper MF74 (2003).

20. S. Xiao, and A. Weiner, "Four-user 3GHz Spaced Subcarrier Multiplexing (SCM) Using Optical Direct-Detection via Hyperfine WDM," IEEE Photon. Technol. **17**, 2218-2220 (2008).
21. S. J. Jansen, I. Morita, N. Takeda, and H. Tanaka, "Optical OFDM. A hype or is it for real?," in Proc ECOC, paper Mo.3.E.3 (2008).
22. J. Gaudette, D. Krause, J. Cartledge, and K. Roberts, "Offset Sideband Modulation at 2.5 GSym/s," in Proc OFC, paper OTHD1 (2007) .

1. Introduction

Orthogonal frequency division multiplexing (OFDM) is in common use for digital video broadcast, DSL and wireless communication systems such as WiFi and WiMAX [1-3]. Recent availability of high speed ADC and DAC, has spurred theoretical and experimental research in optical fiber systems using OFDM (OOFDM) [4-14]. By partitioning high bit rate data onto a large number of subcarriers, OOFDM systems can tolerate large amounts of chromatic dispersion. With the advantages of single tap equalization for dispersion or phase walkoff, and scalable capacity, OOFDM can be used advantageously in applications spanning long-haul to access. Coherent detection OOFDM experiments have achieved more than 4000km transmission at 25.8 Gb/s data rate per wavelength [14]. In the case of 100 GE, a number of techniques have been proposed to increase the OOFDM capacity by integrating multiple OOFDM bands onto an optical carrier or doubling the sampling rate [14-17]. However with conventional double sideband optical modulation, when an OFDM band is upconverted onto an optical frequency, a redundant image band on the other side of the optical carrier will be created and has to be removed by an optical filter. This not only makes the transmitter complicated, it does not make full use of the transmitter bandwidth resource.

In this paper, we propose a cost-effective solution to double OOFDM data rate on each optical carrier. The transmitter uses a conventional dual-electrode MZM. By adding a 90º relative phase shift between RF signals at the two MZM electrodes, two independent OFDM bands can be simultaneously modulated onto the opposite sides of the optical carrier. This doubles the transmission capacity with respect to the available modulation bandwidth of the modulator without requiring an optical filter to generate a single optical sideband. A commercial Nortel eDCO optical transmitter card is used in the experiment. It has a pair of arbitrary waveform generators (AWGs) each with 22Gs/s sampling speed. This transmitter accepts digitally generated OOFDM signals without the need of analog RF synthesizer and mixer. The loop transmissions are conducted for a single OOFDM band and for two independent OOFDM bands simultaneously.

2. Dual-band OFDM transmitter

The proposed dual-band OOFDM transmitter illustrated in Fig.1 comprises both SSB generation of OFDM signals in the RF domain and optical SSB generation [18] using a dual-electrode MZM modulator. The shaded region in Fig.1 shows the block diagram of digital OFDM signal generation accomplished by software programming. Digital data are loaded directly into the arbitrary waveform generators (AWGs) whose outputs drive the two arms of the dual-electrode MZM to construct a spectrum having independently coded OOFDM sidebands on either side of the optical carrier. When compared with usual implementations [10] this effectively doubles the capability of the OOFDM transmitter on existing hardware.

The digital processing block, shown schematically in the grey shaded region of figure 1, represents the functions which execute the desired transmission spectrum. Althought there might be other techniques, we adopt a Hermitian symmetry in designing the OFDM signal [10, 11], so that after IFFT, two real-valued OFDM time domain symbol patterns, A and B are generated. Each OFDM data pattern and its Hilbert transform is upconverted onto a RF carrier f_m with a 90° phase shift. After combination, the up-converted electrical signals a and b are both single-sideband in the frequency domain, and are then combined by a 2 x 2 90° hybrid with a 90° relative phase shift between the RF signals before driving the two MZM electrodes. Since signal a and signal b are both digitally generated, the ideal single-sideband quality can be guaranteed. When the modulator is biased at the quadrature point, another Hilbert

transform is performed, and optical SSB modulation can be achieved as previously demonstrated [19]. Fig.2 illustrates that signal a and b are loaded on the lower and the upper optical sidebands, respectively, and each occupying the opposite side of the RF carrier f_m. RF SSB modulation is essential in this transmitter to minimize the impact of nonlinear mixing while maintaining the optimum optical bandwidth efficiency.
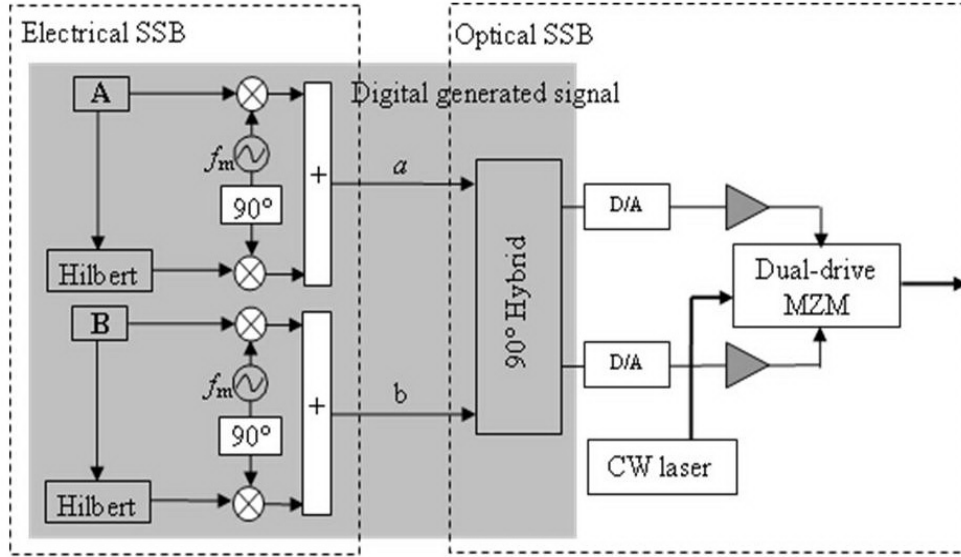

Fig. 1. Transmitter configuration which allows double OFDM sidebands to be created by a simple dual-electrode MZM
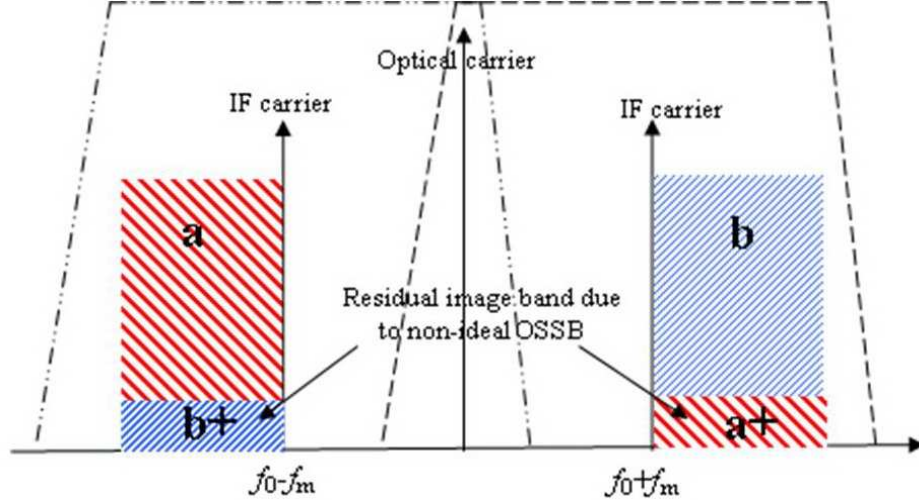

Fig. 2. Illustration of dual OOFDM bands obtained with both RF SSB and optical SSB. Dot-dashed line and dashed line indicate ideal optical demultiplexer transfer function at a direct detection optical receiver.

Since the two OOFDM bands are symmetrically allocated on both sides of the optical carrier, a narrowband optical filter may be required before direct detection to separate these two bands, Crosstalk on each OFDM band is generated by two mechanisms: (1) non-ideal optical SSB in the modulation process, which leaves a weak residual image band; (2) non-

ideal optical demultiplexing at the receiver, so that a small part of the signal from the unwanted sideband may leak to overlaps with the selected sideband in the direct detection process. To address the first mechanism, high quality optical SSB can be achieved by accurately selecting the quadrature bias point of MZM and using a feedback control to optimize the bias. Theoretically, to ensure a 30dB extinction ratio between the wanted and the unwanted sidebands, the bias point needs to be set within ±3.6% of the quadrature point. To address the second issue, the frequency selectivity of the optical filter has to be high enough such as using a hyperfine WDM demultiplexer [20]. In order to avoid intermodulation and harmonic distortions caused by the mixing among subcarriers of the OOFDM band, a guard band at least equal to the OFDM bandwidth has to be reserved between the carrier and the OFDM sideband.

3. Transmission system experimental configuration and results

Figure 3 shows the transmission system experimental setup using the dual-band OOFDM configuration. It consists of the OOFDM transmitter as described above, a fiber-optic re-circulating loop to serve as transmission medium, a direct-detection optical receiver followed by digital scope and off-line digital signal processing. A Nortel eDCO transmitter card [22] was used in the experiment to demonstrate feasibility of the proposed OOFDM transmitter. It has a pair of high-speed AWG's and was developed to enable electrical-domain dispersion pre-compensation in optical systems. Although this eDCO card has up to 22 Gsamp/s AWG speed, the transmission data rate is primarily limited by our LeCroy digital oscilloscope which has a sampling rate of 20GS/s and an approximately analog bandwidth of 6.2GHz. Within these constraints, our experimental system was designed to carry data at 10Gb/s, i.e. 5Gb/s payloads in each of the two OOFDM bands.
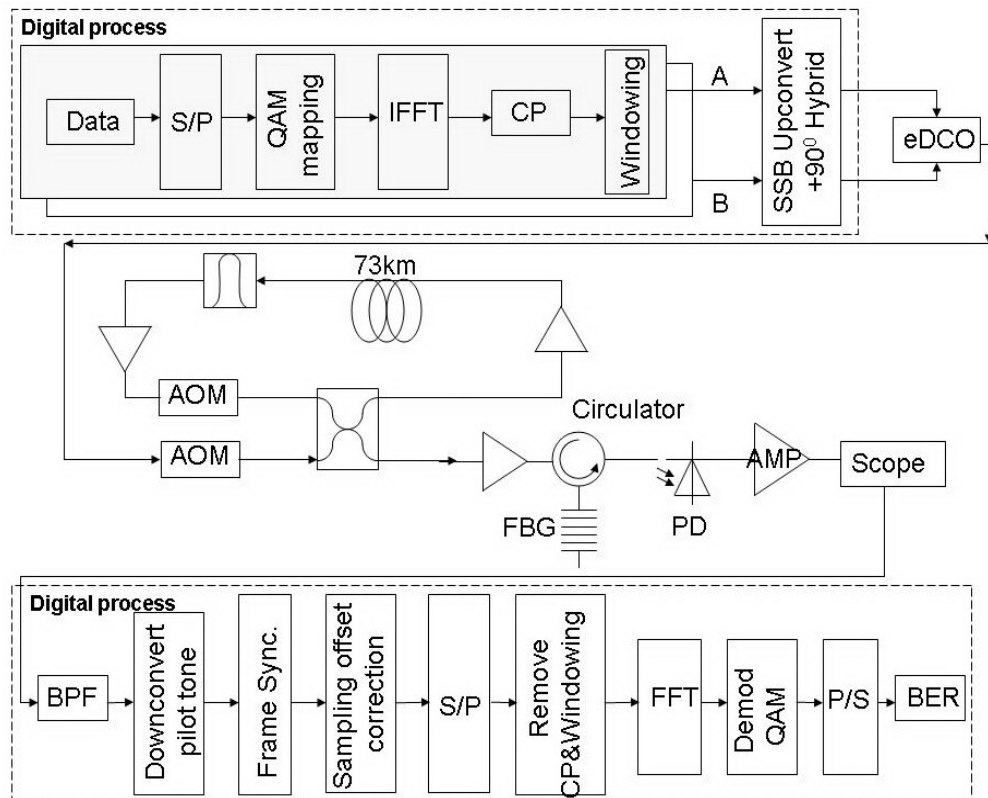

Fig. 3. Block-diagram of the transmission experiment using a dual-band OFDM transmitter.

Two independent PRBS data sequences are quadrature amplitude modulated mapping to a constellation size of 4. For each OOFDM sideband, FFT size of 256 is used and the data is partitioned into 32 subcarriers. The remaining subcarriers are zero padded for oversampling, thus the width of each OFDM sideband is 2.5GHz. In the OFDM frame design, two training symbols are inserted at the beginning of each OOFDM symbol for time synchronization and digital equalization. After IFFT, an OFDM frame pattern of 1.47μs is generated in time domain, and a cyclic prefix of 0.6ns is added to overcome the accumulated chromatic dispersion in the subsequent fiber loop transmission system and to avoid the requirement of optical domain dispersion compensation [21]. Raise cosine windowing in time domain with a roll-off factor of 0.2 is also applied to suppress the OOFDM side lobes. The final OOFDM bandwidth is 3GHz per sideband including the effects of cyclic prefix and widowing. Thus, the OFDM baseband signal is upconverted to an RF carrier f_m = 3GHz. The first subcarrier is zero-padded for Hermitian symmetry and ready for CW component insertion. The CW component corresponds to a 3GHz sinusoid in the IF spectrum and will be used as a pilot tone to facilitate frequency down-conversion [12].

The two generated OFDM signals A and B are digitally manipulated based on the method illustrated in Fig. 1. They are converted into analog signals through AWGs with 6-bit resolution. These electrical signals are amplified to drive the two electrodes of the MZM within the eDCO card. To ensure adequate image sideband suppression, we carefully selected the MZM quadrature bias point. Figure 4 (a) shows the optical spectrum measured by coherent heterodyne detection when there is only a single OFDM band loaded to the optical carrier. An approximately 33dB image band rejection is obtained, which ensures a minimum crosstalk when two OFDM bands are loaded. Figure 4 (b) shows the measured optical spectrum when the two OFDM bands are loaded one either side of the optical carrier. The power of the upper sideband appears approximately 3-dB lower than the lower sideband due to the high frequency roll-off of the RF components in the coherent detection measurement.
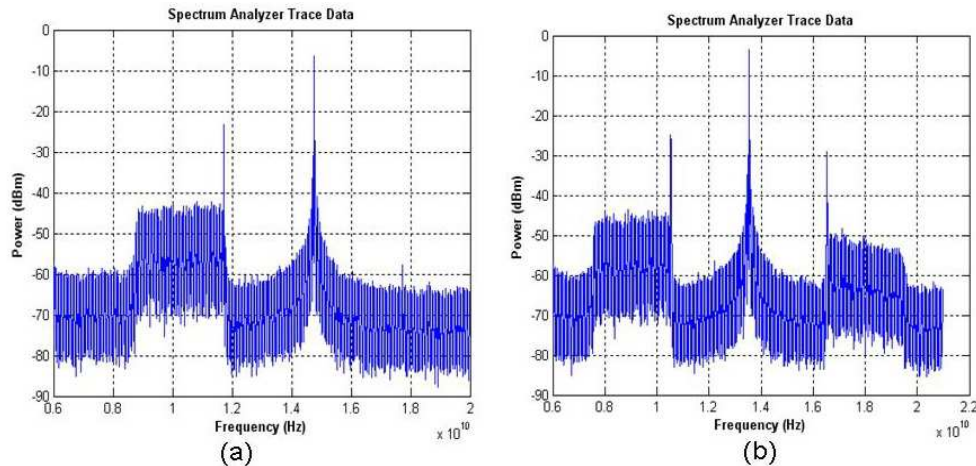

Fig. 4. (a) Optical spectrum of single band OFDM modulation which shows a 33dB image band suppression and (b) Dual-band OFDM optical spectrum

The fiber-optic re-circulating loop contains a 73km span of standard single-mode fiber (SMF) having an accumulated chromatic dispersion of approximately 1240ps/nm and a total loss of 18dB. Two EDFAs are used in the loop one before and one after the SMF to compensate the fiber loss and the additional 10dB loss due to loop switches. A 1nm bandwidth tunable optical filter is used after the first EDFA to suppress the wideband ASE noise. At the output of the re-circulating loop, another low noise EDFA is used to boost the signal optical power before input to the receiver.

A FBG filter with a 3dB bandwidth of 0.08nm is used to select one OFDM band and suppress the other. Since the FBG is not tunable, we adjusted the transmit laser wavelength to match the passband of the FBG and select the desired OFDM band. Figure 5(a) shows the dual-band OFDM optical spectrum measured by an optical spectrum analyzer (OSA) with and without FBG filtering. Figure 5(b) displays the filtered optical spectrum measured by coherent heterodyne detection. In this figure the rejection of the unwanted OFDM band by the FBG is seen to be approximately 20dB. In the direct detection receiver, a wideband photodetector followed by a low noise RF amplifier are employed. A LeCory 8600A digital oscilloscope performs digital sampling and data storage. In the off-line digital signal processing, the signal first passes through a bandpass filter to eliminate the wideband noise. The OFDM signal is then downconverted from the IF band to baseband by mixing with the complex conjugate of the pilot tone at 3GHz which is extracted by a digital filter. The pilot tone power and the digital filter bandwidth were chosen to minimize phase noise. After FFT, the cyclic prefix and windowing samples are removed. The subcarrier channels are demodulated separately to recover the original 2^{13}-1 PRBS bits streams, and the bit error rate (BER) is evaluated.
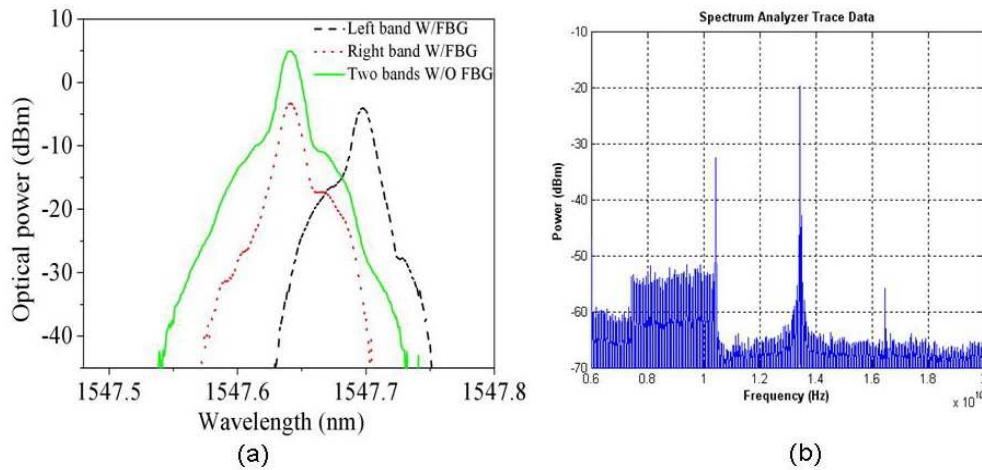

Fig. 5. (a) Optical spectrum measured by an OSA for dual-band OFDM signal and the spectra filtered by an FBG (b) Optically filtered spectrum measured by coherent detection

To quantify the transmission performance of this dual-band OOFDM system, we first measured a simple system with only one OOFDM band on the optical carrier, and no FBG filter at the receiver. ASE noise loading was used to evaluate back to back transmitter and receiver performance. Fig. 6 a) shows the measured BER as the function of optical signal-to-noise ratio (OSNR) with two different modulation index defined as RF_{p-p}/V_π. It shows that the system performance improve with increasing modulation index (even for indices greater than 100%). This behavior demonstrates that the system is primarily noise limited. As the maximum RF voltage has low probability of occurrence, it allows the use of high modulation indices, which improves the OSNR for the majority of data bits. However, increasing the modulation index beyond 1.5, leads to a rapid BER deterioration as the effects of power clipping become overwhelming. It needs to note that this dual optical sideband system has a relatively large optical carrier; it requires higher OSNR at the receiver. Our computer simulation indicated that an OSNR of approximately 17dB (for 0.1nm noise bandwidth) is required to achieve 10^{-3} BER. This is about 7dB worse compared to a system using only one optical sideband [13].

We applied inversed nonlinear transfer function of the MZM on digital modulating signal for MZM nonlinear pre-compensation. However, since the generated mixing noises are filtered out in post digital processing and second harmonic terms are cut off by the 6GHz bandwidth of this oscilloscope, this system is primarily ASE noise limited. Therefore we did not find noticeable performance improvement through pre-compensation in our experiment.
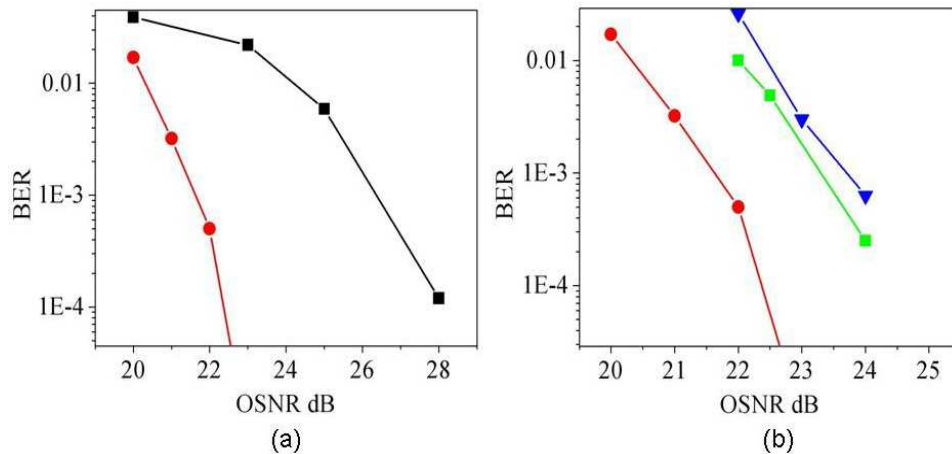
Fig. 6. (a) Measured BER versus OSNR for single-band OFDM transmitter back-to-back with modulation indices of m = 1.5 (solid circle) and m = 1.25 (diamond). (b) BER versus OSNR for single OFDM bands without FBG (solid circle), single OFDM bands with FBG at the receiver (diamond) and double OFDM bands with FBG at the receiver (solid triangles). OSA resolution is 0.1nm.

Secondly, we added the second OFDM sideband and the FBG filter at the receiver. The system penalty due to optical filtering and the crosstalk between the two sidebands is further characterized. Figure 6(b) shows the measured BER versus OSNR with the modulation index of 1.5. Adding the receive FBG filter to the single sideband OOFDM system (solid circles) leads to an OSNR penalty of ~ 1.5 dB. Since the passband of this particular FBG is not flat enough within the signal OFDM band, and it also partially cuts off the carrier power, this 1.5dB OSNR penalty is mainly attributed to the non-ideal transfer function of the FBG, which in principle can be reduced by better filter design. When the second OFDM sideband is added, a penalty of less than 0.5dB OSNR stems from the crosstalk between the two OFDM sidebands.
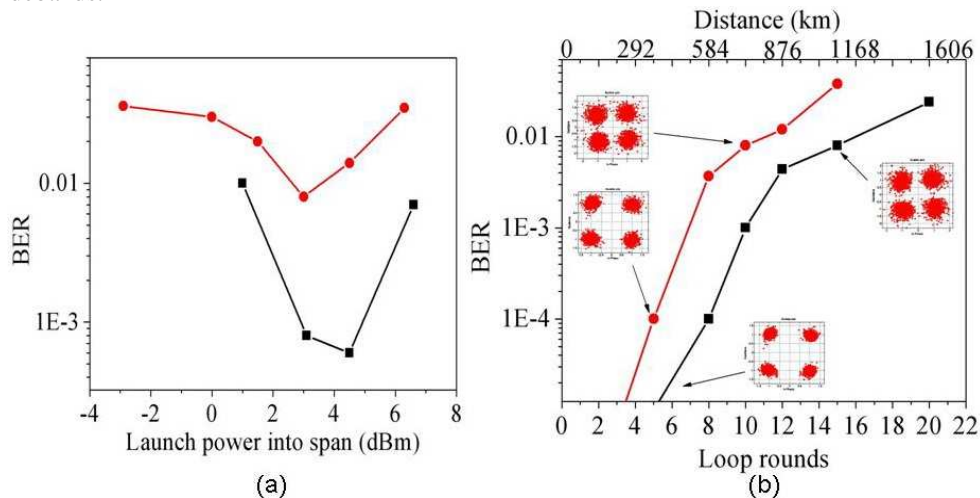

Fig. 7. (a) BER versus launched optical power after 10 circulations in the loop for systems with single-band (diamonds) W/O FBG and double-band (solid circles) W FBG. (b) BER versus the number of loops for systems with single-band (diamonds) W/O FBG and double-band (solid circles) W FBG. Loop span length 73km.

Results from the re-circulating loop experiment with the single and dual band optical signal are shown in Fig. 7, where the single-band system does not have a FBG filter at the receiver. Figure 7(a) shows the measured BER after 10 circulations in the re-circulating loop as the function of the signal optical power launched into the transmission fiber in the loop. The optimal optical power level for the double band situation is approximately 1dB lower than that with single OFDM band mainly due to additional nonlinear crosstalk introduced between the two bands at higher powers. Figure 7(b) shows the BER versus the number of loops for single and double OFDM sidebands, respectively. The optical power launched into the fiber was optimized based on a 10-loop system. The insets in Fig. 7(b) show constellation diagrams after specific loops. To achieve the comparable BER performance, the maximum transmission distances of the system with double OFDM sidebands are approximately 400km shorter than the system with a single OFDM sideband. Again, this discrepancy is mainly attributed to the OSNR penalty introduced by the FBG filter at the receiver as discussed above.

4. Conclusion

We have demonstrated an OOFDM transmitter based on both SSB RF modulation and tandem SSB optical modulation. The SSB RF modulation was digitally generated, whereas the optical SSB modulation was created using a simple dual-electrode MZM, which simultaneously delivers two independent OFDM sidebands, one on each side of the optical carrier. This allows the doubling of transmission capacity compared with standard optical SSB technique. We utilized a commercial eDCO optical transmitter card to demonstrate the feasibility of this dual-band OFDM concept. Long-distance optical transmission experiment using 10Gb/s data rate has been conducted using a fiber-optic re-circulating loop. The impacts of modulator biasing, modulation index and the impact of crosstalk between the two OOFDM bands were discussed. Since this transmitter is capable of delivering a much higher data rate (>20Gb/s), if a digitizing oscilloscope with higher sampling rate is available, this technique should be able to provide a system capacity of above 20Gb/s on each optical carrier.

Acknowledgements